ORSGET

Where faults meet: palaeostress analysis at the juncture of the Concud and Teruel faults

P. Lafuente[1*] and L. Arlegui[1]

[1]*Departamento de Ciencias de la Tierra, Universidad de Zaragoza. C/Pedro Cerbuna, 12, 50009 Zaragoza, Spain.*

[*]e-mail: palomalt@unizar.es

Abstract: Put into context within the framework of recent palaeostress surveys around the Concud fault, this paper shows the results of stress inversion from fault populations within the juncture region of the Concud and Teruel faults. They indicate that the junction of these major faults is a place for phenomena of stress perturbation where each fault alternates to dominate and produce minor fractures, instead of creating an averaged stress field.

Keywords: Iberian Chain, Neogene-Quaternary extension, normal fault, stress inversion, Concud fault, Teruel fault.
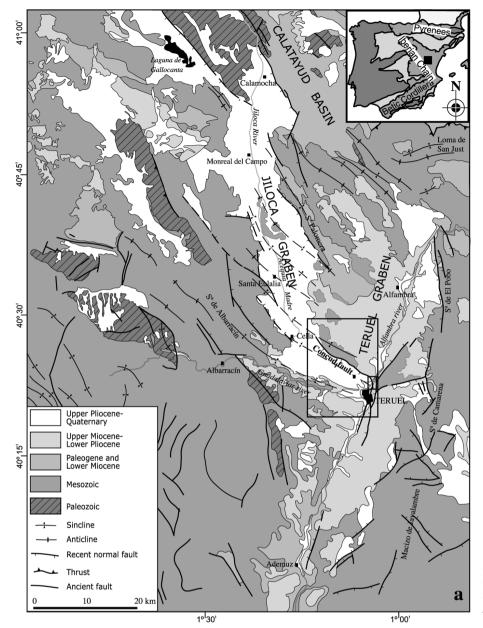
The main Neogene-Quaternary extensional episodes of the Iberian Chain have been thoroughly studied in the past few years, including the use of palaeostress inversion techniques to characterise the involved stress fields and how they evolved. The aim of this paper is to further explore, within this regional context, the palaeostress behaviour of minor faults within the narrow region where large oblique normal faults belonging to different sets meet.

Geological setting

The Iberian Chain forms a NW-SE-striking intraplate fold belt located in eastern central Spain and developed as a consequence of the Mesozoic Iberian Basin inversion. The Neogene-Quaternary extension (Capote *et al.*, 2002) produced a network of extensional faults in two main directions: NNE-SSW-striking faults as at the boundaries of the Teruel and eastern Maestrazgo grabens; NW-SE-striking faults such as those at the eastern limit of the Jiloca graben. This extensional fault network was built in two successive stages (Late Miocene and Plio-Pleistocene in age). The first episode produced the NNE-SSW structures whereas the second stage represents the Jiloca semigraben creation

(with an overall NNW-SSE strike) and the reactivation of the Teruel semigraben.

The eastern boundary of the Teruel semigraben is constituted by several N-S to NNE-SSW normal faults, the Teruel fault being the main structure (Fig. 1). The semigraben is filled by Neogene continental deposits (mud-flat deposits and lacustrine carbonates and evaporites) with lateral and vertical changes and up to 400-500 m in thickness. There are also alluvial fans developed from the basin margin (Anadón and Moissenet, 1996; Alonso-Zarza and Calvo, 2000). The exorreism and the deposition of red clastic materials began as a consequence of the reactivation of the structures and climate changes in the Upper Pliocene (Moissenet, 1982; Gutiérrez *et al.*, 1996). During the Pleistocene, the development of pediments and fluvial terraces continued.

The Jiloca graben (Figs. 1 and 2), a NNW-SSE structure, shows an eastern boundary conformed by three en echelon normal faults (Calamocha, Sierra Palomera and Concud). The filling of the semigraben consists of Upper Pliocene and Pleistocene materials, represented by red clastic deposits of small alluvial fans and glacis,

Figure 1. Location of the studied area. Rectangles correspond to figures 2 and 4. Modified from Arlegui *et al.* (2006).

only several tens of meters in thickness, overlying unconformably the Teruel graben fill. Both semi-grabens, Jiloca and Teruel, meet near the city of Teruel through the juncture of the Concud and Teruel faults.
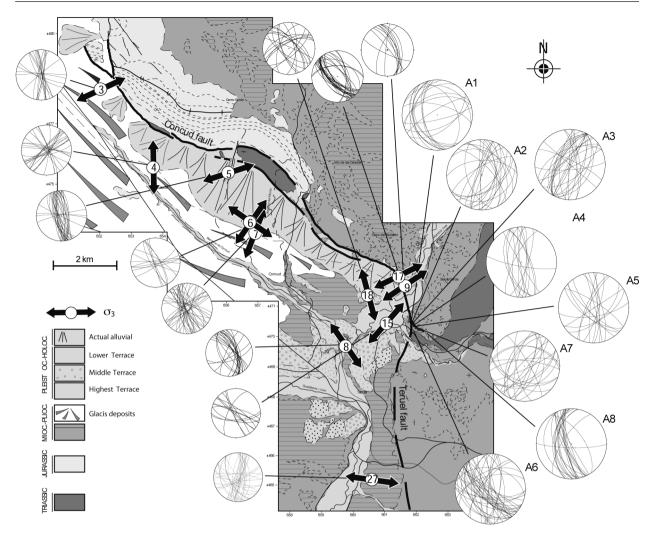
Stress inversion methodology

For the analysis of striated fault populations a sequence of three methods has been used to analyse the data (Fig. 3):

Right Dihedra method (Pegoraro, 1972; Angelier and Mechler, 1977). This simple geometrical method provides an initial estimation of stress directions.

y-R diagram (Simón, 1986). In this method one of the principal stress axes is supposed to be vertical, and tensors may be represented by only two parameters on a 2D approximation: y (azimuth of the maximum horizontal stress, σ_y) and R (stress ratio in Bott's equation (Bott, 1959), R = $(\sigma_z-\sigma_x)/(\sigma_y-\sigma_x)$). The y-R pairs satisfying one individual fault give rise to a curve. The 'knots' where the curves intersect indicate a preliminary spectrum of all possible solutions and their relative importance in the fault population.

Etchecopar's method (Etchecopar *et al.*, 1981; Etchecopar, 1984). This is a numerical method

Figure 2. Geological map of the Concud and Teruel faults with results of previous palaeostress analysis. Arrows and small stereoplots: local directions of σ_3 axes and faults collected at each site; data obtained from Simón (1989), Simón and Soriano (1993), Cortés (1999), and Arlegui *et al.* (2005, 2006). Large stereoplots: new faults collected at each site for this analysis.

that generates a complete solution (3D orientation of the three principal stress axes and stress ratio). With this method it is possible to explore the solutions suggested by the Right Dihedra and y-R diagrams to constrain the final solution. Based upon the minimization of the angles between real and theoretical striations, it allows the separation of different stress tensors by means of an adequate management of the percentage of data submitted to minimization.

In cases where striation is not present, but it is possible to determine the sense of slip, we used the method of stress inversion proposed by Lisle *et al.* (2001) based only on fault plane orientation and slip sense. This method is based on the fact that the dip-slip component of a fault with dip angle γ indicates the sign of the gradient of the normal stress σ/γ. If this information is available for differently oriented fault planes (newly formed or reactivated), the orientation of principal stress axes can be constrained. The method involves a comparison of the normal stress levels calculated for the observed fault with that calculated on a slightly steeper-dipping imaginary fault plane. A grid search method then allows compilation of all stress tensors compatible with the observed faults and their respective slip senses. Usually, a high number of compatible stress solutions are found. Modal orientations of the respective principal stress axes are represented on stereoplots, while stress ratios ($R = (\sigma_z - \sigma_x)/(\sigma_y - \sigma_x)$) are usually displayed on a frequency histogram.

a

b

σ_1: 200,79
σ_2: 001,10
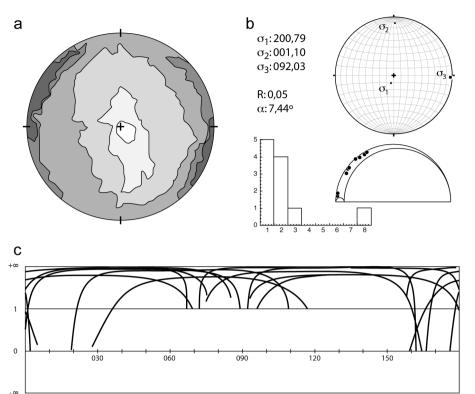σ_3: 092,03

R: 0,05
α: 7,44°

c

Figure 3. Graphic expression of the results obtained with applied methods. (a) Right Dihedra method (Pegoraro, 1972; Angelier and Mechler, 1977), (b) y-R diagram (Simón, 1986), (c) Etchecopar's method (Etchecopar et al., 1981; Etchecopar, 1984). Example of station A4.
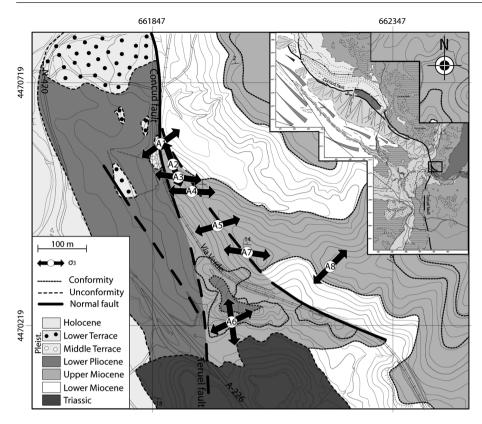
Palaeostress results and discussion

Previous papers indicate that the regional stress field is basically a multidirectional tension (vertical σ_1, $\sigma_2 \sim \sigma_3$) with a preference for primary ENE-WSW to NE-SW-trending σ_3 trajectories. This field was driven by a combination of intraplate remote compression, rifting and crustal uplift (Simón, 1989; Arlegui et al., 2005, 2006). This stress field is locally perturbed by the Concud fault (Arlegui et al., 2006). The σ_3 trajectories are deflected to become either parallel or perpendicular to the fault strike; and there is a tendency for σ_2 and σ_3 axes to switch. These features are easily explained by theoretical models of stress perturbation within an extensional regime (Simón et al., 1988; Kattenhorn et al., 2000). The area around the Teruel fault has been subject to similar studies (Simón, 1989; Cortés, 1999; Arlegui et al., 2005), indicating a similar stress field, ENE-WSW-trending σ_3 directions, parallel to those of the Concud fault, or either parallel or perpendicular to the Teruel fault.

The research of the area between the Concud and Teruel faults involved the sampling and analysis of eight new fault populations and the comparison of the results with previous studies. The new sites include 166 minor scale normal faults, showing dip separations in the range of centimetres. The sense of

displacement was determined by the direct observation of stratigraphical markers, or by finding kinematic indicators. The newly obtained palaeostress results are summarised in table 1 and figure 4. Figure 2 covers a broader region and offers a more general view of the palaeostress setting along the Concud fault, including previously published results (Simón, 1989; Simón and Soriano, 1993; Cortés, 1999; Arlegui et al., 2005, 2006). In both maps (Figs. 2, 4) the arrows indicate the modal azimuth of the obtained σ_3 axes at each site.

Sites 1 through 5 and 7 to 8 are located on a ridge of densely fractured Miocene limestone overlooking the "Vía Verde" tourist track. Site 6 lies in a derelict gypsum quarry, located south of the "Vía Verde" and north of the A-226 road (Fig. 4).

The collected fault measurements show some variability in disposition, though some common features can be detected. Some sites (A1, A3, A7) include faults from at least two sets with mutually perpendicular strikes, though a dominant set is quite often identifiable. Others (A4, A8) present a single fault set. Finally, there are fault populations (A6, A2) composed of two sets of oblique strike. The most common averaged strikes are NNW-SSE, NNE-SSW, NW-SE and E-W. Fault dips have a bimodal distribu-

Figure 4. Geological map of the juncture of Concud and Teruel faults with results of palaeostress analysis. Arrows: local directions of σ_3 axes.

tion, with two maxima at 55° and 75°. The rake of the striae is on average rather steep, with a maximum around the 80-85° mark; it is important, as we will see later, to point out that some fault surfaces have two different striae, typically one of them is rather steep (even near vertical) while the other is of a gentler rake. The described faults are perfectly similar to faults of the same size found all around the Neogene-Quaternary extensional major structures. Nonetheless, the density of faults, especially at site 6, is notably higher than in other areas.

Table 1 summarizes the results of the stress inversion procedures. As expected, the stress field recorded in this fault population can be considered as a multidirectional tension (near vertical σ_1, $\sigma_2 \sim \sigma_3$) as the low stress ratios, R_e, clearly show. The azimuths of σ_3 are either around E-W (A3, A4, and A7), or around NE-SW (A1, A2 by stress axes swapping, A5, A6 and A8). Figure 4 shows how we can identify two tendencies in our solutions by comparing the stress azimuths with both major faults. First, all results can be seen as a σ_3 perpendicular to a major fault. Thus such is the case for sites A1, A5, A6 and A8, where they are perpendicular to the nearest major fault; in the case of A1, the azimuth of the obtained σ_3 is perpendicular to the eastern branch of the Concud fault, whereas A5 shows a similar disposition with the western branch. This suggests that both

branches were similarly active at the time of faulting. Site A8 has a σ_3 perpendicular to the trace of the Concud fault in its eastern end, where the fault recovers to some extent its overall NW-SE to WNW-ESE strike. Site A6 is somewhat more special than the others. First, it corresponds to the area with the highest density of fractures. Second, it is located near the probable mark of the major faults juncture. Finally, we obtain two different stress solutions at this site, each of them explaining a separate striation when double striae are present in a given fault surface. One of the solutions is almost parallel to the strike of the Teruel fault; a phenomenon easily understood when we check the stress ratio. The most probably solution represents a case of stress swapping between σ_2 and σ_3. The second solution is compatible with the general disposition of the Concud fault some hundreds of metres NW.

Site A2 represents a second case of stress swapping; again, a low stress ratio allows the swap of σ_2 and σ_3. Thus, site A2 would be interpreted as near perpendicular to the Concud fault, with a gentle stress deflection due to the close vicinity of both branches of the Concud fault.

Sites A3, A4 and A7, with a σ_3 azimuth around E-W to ESE-WNW are most probably recording the stress field related to the Teruel fault.

Station	Lithology	Age	No. of faults	σ_1	σ_3	R_e
A1	Limestone	Late Miocene	15	319, 64	056, 03	0.32
A2	Limestone	Late Miocene	9	323, 83	160, 06	0.01
A3	Limestone	Late Miocene	16	190, 90	098, 00	0.00
A4	Limestone	Late Miocene	11	200, 79	092, 03	0.05
A5	Limestone	Late Miocene	18	256, 34	074, 25	
A6	Limestone and gypsum	Late Miocene	48	176, 72 311, 66	352, 18 064, 10	0.00 0.02
A7	Limestone	Late Miocene	24	179, 88	278, 04	0.03
A8	Limestone	Late Miocene	25	090, 82	225, 06	0.04

Table 1. Results of palaeostress analysis. Station 5 was analysed with the Dip Slip (Lisle *et al.*, 2001) stress inversion program.

Conclusions

The general features observed at the neighbourhood of the Concud faults in previous research are also present when we examine the Concud-Teruel juncture: minor normal faults of centimetre scale displacement that reflect a multidirectional tension (vertical σ_1, $\sigma_2 \sim \sigma_3$) stress field: the recorded stress solutions share, at all sites, the multidirectional character of the regional tensors, in some cases to the extent of having a stress ratio of zero. This close to the major faults, however, the ENE-SWS strike of the remote stress field was mostly obliterated by stress perturbations, akin to the above mentioned for the broader regional survey, albeit more remarkable. Thus, the obtained stress solutions correspond either to the σ_3 axis deflected to become perpendicular to the major fault, or deflected and/or swapped to become parallel.

Acknowledgements

References

ANADÓN, P. and MOISSENET, E. (1996): Neogene basins in the Eastern Iberian Range. In: P. F. FRIEND and C. J. DABRIO (eds): *Tertiary basins of Spain.* Cambridge University Press: 68-76.

ANGELIER, J. and MECHLER, P. (1977): Sur une méthode graphique de recherche des contraintes principales également utilisable en tectonique et en séismologie: la méthode des dièdres droits. *B. Soc. Geol. Fr.*, 19, 7: 1309-1318.

ALONSO-ZARZA, A. M. and CALVO, J. P. (2000): Palustrine sedimentation in an episodically subsiding basin: the Miocene of the northern Teruel Graben (Spain). *Palaeogeogr. Palaeoclim. Palaeoecol.*, 160: 1-21.

ARLEGUI, L. E., SIMÓN, J. L., LISLE, R. J. and ORIFE, T. (2005): Late Pliocene-Pleistocene stress field in the Teruel and Jiloca grabens (eastern Spain): contribution of a new method of stress inversion. *J. Struct. Geol.*, 27: 693-705.

ARLEGUI, L. E., SIMÓN, J. L., LISLE, R. J. and ORIFE, T. (2006): Analysis of non-striated faults in a recent extensional setting: the Plio-Pleistocene Concud fault (Jiloca graben, eastern Spain). *J. Struct. Geol.*, 28: 1019-1027.

BOTT, M. H. P. (1959): The mechanics of oblique fault slip. *Geol. Mag.*, 96: 109-117.

CAPOTE, R., MUÑOZ, J. A., SIMÓN, J. L., LIESA, C., and ARLEGUI, L. E. (2002): Alpine tectonics I: The Alpine system north of the Betic Cordillera. In: W. GIBBONS and M. T. MORENO (eds): *The geology of Spain*, Geol. Soc. London, 367-400.

CORTÉS, A. L. (1999): *Evolución tectónica reciente de la Cordillera Ibérica, Cuenca del Ebro y Pirineo centro-occidental*. PhD Thesis, University of Zaragoza, 409 pp.

ETCHECOPAR, A. (1984): *Etude des états de contraintes en tectonique cassante et simulations de déformations plastiques (approche mathématique)*. PhD Thesis, USTL Montpellier, 270 pp.

ETCHECOPAR, A., VASSEUR, G. and DAIGNIÈRES, M. (1981): An inverse problem in microtectonics for the determination of stress tensors from fault striation analysis. *J. Struct. Geol.*, 3: 51-65.

GUTIÉRREZ, F., GRACIA, F. J. and GUTIÉRREZ, M. (1996): Consideraciones sobre el final del relleno endorreico de las fosas de Calatayud y Teruel y su paso al exorreísmo. Implicaciones morfo-estratigráficas y estructurales. In: A. GRANDAL and J. PAGÉS (eds): *IV Reunión de Geomorfología*, Sociedad Española de Geomorfología, O Castro (A Coruña): 23-43.

KATTENHORN, S. A., AYDIN, A. and POLLARD, D. D. (2000): Joints at high angles to normal fault strike: an explanation using 3-D numerical models of fault-perturbed stress fields. *J. Struct. Geol.*, 22: 1-23.

LISLE, R. J., ORIFE, T. and ARLEGUI, L. E. (2001): A stress inversion method requiring only fault slip sense. *J. Geophys. Res.*, 106, B2: 2281-2289.

MOISSENET, E. (1982): Le Villafranchien de la région de Teruel (Espagne). Stratigraphie-deformations-milieux. *Collòque «Le Villafranchien Méditerranéen»*, Lille: 229-253.

PEGORARO, O. (1972): *Application de la microtectonique à un étude de neotectonique. Le golfe Maliaque (Grèce centrale)*. Thèse IIIème cycle, *USTL Montpellier*, 41 pp.

SIMÓN, J. L. (1986): Analysis of a gradual change in stress regime (example from the eastern Iberian Chain, Spain). *Tectonophysics*, 124: 37-53.

SIMÓN, J. L. (1989): Late Cenozoic stress field and fracturing in the Iberian Chain and Ebro Basin (Spain). *J. Struct. Geol.*, 11: 285-294.

SIMÓN, J. L., SERÓN, F. J. and CASAS, A. M. (1988): Stress deflection and fracture development in a multidirectional extension regime. Mathematical and experimental approach with field examples. *Ann. Tectonicae*, II, 1: 21-32.

SIMÓN, J. L. and SORIANO, M. A. (1993): La falla de Concud (Teruel): actividad cuaternaria y régimen de esfuerzos asociado. In: *El Cuaternario en España y Portugal.* Actas 2ª Reunión del Cuaternario Ibérico, 2: 729-737.